COOLING AND PACKAGING OF ACCUMULATORS FOR FORMULA

SAE ELECTRIC CAR

by

YIN, HANG

Presented to the Faculty of the Graduate School of

The University of Texas at Arlington in Partial Fulfillment

of the Requirements

for the Degree of

MASTER OF SCIENCE IN MECHANICAL ENGINEERING

THE UNIVERSITY OF TEXAS AT ARLINGTON

May 2016

Acknowledgements

I would like to express my deepest gratitude to my advisor Dr. Woods at University of Texas at Arlington who is also the team advisor of UTA Racing for his humorous and inspirational teaching in class, for encouraging me to extend my knowledge beyond textbooks and for offering us the greatest opportunity of working as a team.

I would like to thank my friend Michael Hibbard who is the Chief Technical of our E-car team. His fearlessness inspires me to be more creative in designing. Many thanks to my teammates David Campbell, Naima Rivas, Audrey Porter and others that helped me in researching my project, learning the electrical aspects of my system and also practicing English.

I would also like to thank my parents for supporting me to study abroad and encouraging me to take on challenges.

April 15th, 2016

iii

Abstract

COOLING AND PACKAGING OF ACCUMULATORS FOR FORMULA

SAE ELECTRIC CAR

Hang Yin, MS

The University of Texas at Arlington, 2016

Supervising Professor: Robert L Woods

Electric car is the future of automotive industry. The performance of the batteries is vital for that of electric cars. Overheating will compromise the performance of batteries, shorten the life span and even damage the battery permanently. So it is crucial to have an efficient packaging and cooling method. This project using Formula SAE Electric car as the testing ground is dedicated to develop the efficient way of thermal and electronic packaging of accumulators for automobiles.

Table of Contents

List of Illustrations

List of Tables

Chapter 1

Introduction

1.1 Introduction to Formula SAE Electric

Formula SAE is an international collegiate competition organized by Society of Automotive Engineers. Students are offered the great opportunity of designing, manufacturing an open wheel race car and competing in both static and dynamic events. Formula SAE has evolved from a domestic event in the U.S. to an international competition throughout the world being held by countries in Europe and Asia.

Electric car is shifting the future of the automotive industry and Formula SAE is no exception for that matter. Formula Student Electric, Figure 1-1, started in Germany long after the first Formula SAE combustion competition, however it is developing rapidly surpassing combustion cars in countless performance records demonstrating significant potential of electric cars in the automotive and motorsport industry.

Figure 1-1 Formula Student Electric Logo

1.2 Introduction to UTA Racing E-16

Figure 1-2 UTA Racing E-16

UTA Racing has been participating in Formula SAE for over thirty years since the very first competition. The team is composed of students from University of Texas at Arlington of many majors including Mechanical Engineering, Aerospace Engineering and Electrical Engineering.

With our proud history and huge expectation we are building our first ever electric car E-16, shown in Figure 1-2, which will compete in Formula Student Electric in 2016. E-16 has an all-wheel drive system consisting of four in-wheel motors with total power of 75 kW which will be the most powerful car in UTA Racing history.

Chapter 2

Thermal Analysis

2.1 Introduction to LFP Battery

The nominal tractive system voltage of E-16 is 198 VDC provided

by 120 Lithium-ion phosphate battery cells, shown in Figure 2-1,

connected in series. Battery cells are provided by team sponsor A123.

Figure 2-1 Lithium-ion Phosphate Battery Cell

There are different types of batteries on the market. We choose

Lithium-ion phosphate battery for the following advantages. First of all, it

does not need prolonged charging when it is new, one regular charge

would be sufficient. Second, the self-discharge of this kind of battery is

relatively low compare to nickel- based batteries. And also, there is no

periodic discharge required and no memory effect which means longer life

span and low maintenance [1] [2].

2.2 Battery Pack

In order to conduct heat out of the batteries and increase the surface area of heat convection, corrugation aluminum is placed between the battery cells serving as heat sinks for every battery pack designed by Michael Hibbard (UTA), as shown in Figure 2-2. The cooling method used is forced convection with a single fan at the exit of the airflow for every three battery packs in each container. Each battery pack is consist of 10 battery cells connected in series. There are total six battery packs being cooled by two fans.

Figure 2-2 Battery Pack

In order to keep the voltage down to under 200V, for each battery pack every two cells will be connected in parallel to from a conjoined cell and every conjoined cell will be connected in series. Therefore for every

two adjacent cells two positive poles will be joined together and same with the negative poles. Then between joined cells the positive pole will be joined to negative pole to form series connect them in series shown in Figure 2-3.

Figure 2-3 SolidWorks Model of Battery Pack
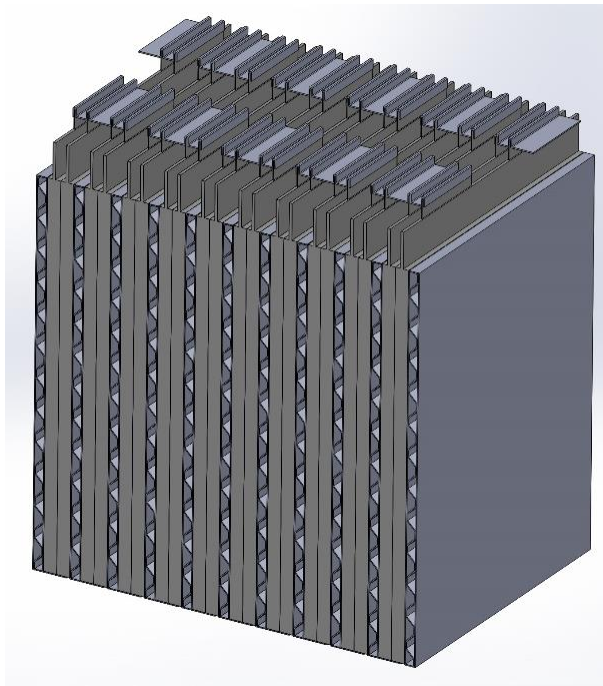
2.3 Battery Heat Dissipation

During discharging the batteries generate enormous amount of heat which needs to be removed to keep batteries from overheating. Assuming all the heat generated by the batteries will be absorbed by air and all the heated air will be removed by fans, as long as enough amount of air is removed in certain amount of time the batteries won't exceed their

optimal operating temperature. Using equation (2.1) the Mass Flow Rate

can be obtained. Mass Flow Rate needed for three battery packs is

0.06kg/s which is equivalent to volumetric flow rate of 127.14 CFM when

heat being generated at 1200W [2] [3]. The day time average high

temperature in Hockenheim Germany is 25°C. And the highest cell

temperature allowed by the competition rule is 60°C [4]. In the calculation

the inlet temperature is chosen as 30°C which is higher than the actual

ambient temperature at the competition, and the outlet temperature is

chosen as 50°C which is lower than the rule requirement. Therefore we

have safety margin on both ends.

Mass Flow rate $\qquad$ $\dot{m} = \dot{Q}/[C_p(T_{out} - T_{in})]$ $\qquad$ (2.1)

Table 2-1 Heat Dissipation

	Symbol	Value	Unit
Heat Dissipation of three packs	$\dot{Q}$	1200	W
Inlet Temperature	T_{in}	30	°C
Outlet Temperature (highest operating temp of the battery)	T_{out}	50	°C
Specific Heat of Air	C_p	1000	J/(kg°C)
Density of Air at 70°C	ρ	1	kg/m^3
Mass Flow Rate	$\dot{m}$	0.06	kg/s
Volumetric Flow Rate	$\dot{V}$	0.06	m^3/s
Volumetric Flow Rate	$\dot{V}$	127.14	CFM(ft^3/min)

2.4 System Resistance of Battery Packs

As the word implies, system resistance is an obstruction to movement, in this case it is the airflow. The static pressure drop is forming with the increase of volumetric flow rate which represents how much resistance an air flow must overcome in order to achieve the desired flow rate. The system resistance curve can be generated either by empirically measuring the static pressure drop using a wind tunnel or by numerical calculation. In this article both methods are being used to ensure the most accurate results.

The static pressure drop is based upon the geometric feature of the flow area and the distance that the airflow has to travel. In this system, the flow path is consist of 264 channels with a trapezoid shape shown in Figure 2-4.
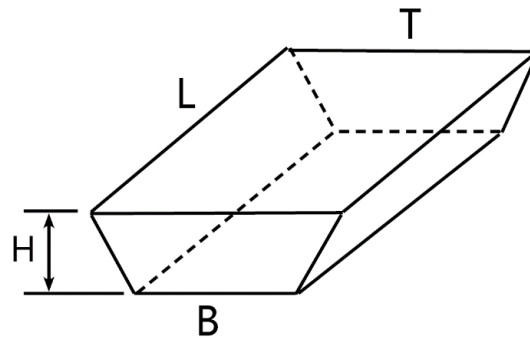
Figure 2-4 Trapezoidal Channel

Table 2-2 shows the geometry used for calculating the static pressure drop.

Table 2-2 Geometry of Trapezoidal Channel

T	12.32	mm
H	4.47	mm
B	3.38	mm
L	160	mm

Flow in a tube can be laminar or turbulent, depending on the flow conditions. Fluid flow is streamlined and thus laminar at low velocities, but turns turbulent as the velocity is increased beyond a critical value. Transition from laminar to turbulent flow does not occur suddenly; rather it occurs over some range of velocity where the flow fluctuates between laminar and turbulent flows before it becomes fully turbulent. For flow in a tube or a pipe the Reynolds number is defined as equation (2.2) where V_e is the fluid velocity, D_h is the hydraulic diameter of the tube, and $v = \mu/\rho$ is the kinematic viscosity of the fluid [2], values shown in Table 2-3.

Reynolds number $$R_e = \frac{\rho\, V_e\, D_h}{\mu} = \frac{V_e\, D_h}{v}$$ (2.2)

Table 2-3 Ambient Parameters

	Symbol	Value	Unit
Kinematic Viscosity of Air	v	0.0002	m^2/s
Viscosity of Air	μ	0.00002	N.s/m²
Density of Air	ρ	1	kg/m³

For flow through noncircular tubes, in this case trapezoidal tube, the Reynolds number is based on the hydraulic diameter D_h defined as equation (2.5) where A is the cross sectional area of the tube and p is the perimeter of the tube, shown in equation (2.3) and (2.4).

Flow Area
$$A = \frac{1}{2} H (B + T)$$
(2.3)

Wetted Perimeter
$$P = B + 2(\sqrt[2]{[\frac{1}{2}(T - B)]^2 + H^2})$$
(2.4)

Hydraulic Diameter
$$D_h = \frac{4A}{P}$$
(2.5)

It certainly is desirable to have precise values of Reynolds numbers for laminar, transitional, and turbulent flows, but this is not the case in practice. Under most practical conditions, the flow in a tube is laminar for Re < 2300, turbulent for Re > 10,000, and transitional in between.

Reynolds numbers can be calculated for given velocities. Also, volumetric flow rate can be calculated using velocity times total flow area for all 264 trapezoidal tubes which is 0.0099 m^2. Table 2-4 shows the Reynolds numbers for each given velocity and volumetric flow rate. The Reynolds number increases with velocity. According to Table 2-1 the least required volumetric flow rate is 127.14 CFM, where the Reynolds number is 2727.27 which indicates the flow is transitioning from laminar to turbulent.

Table 2-4 Reynolds Numbers

Volumetric Flow Rate (CFM)	Velocity (m/s)	Reynolds Number
21.19	1	400
42.38	2	900
63.57	3	1300
84.76	4	1800
105.95	5	2200
127.14	6	2700

In transitional flow, the flow switches between laminar and turbulent randomly. It is known that laminar flow can be maintained at much higher Reynolds numbers in very smooth pipes by avoiding flow disturbances and tube vibrations. In such carefully controlled experiments, laminar flow has been maintained at Reynolds numbers of up to 100,000 [2]. In this system the tubes are formed by Aluminum 6061 T4 with surface roughness between 0.001 mm and 0.002 mm, which is qualified as a smooth surface. And also considering the Reynolds number is much closer to laminar than to turbulent, the airflow in this system will be considered laminar for calculations.

Pressure drop is the quantity directly related to the power requirements for a cooling fan. The pressure drop for a laminar flow in smooth noncircular pipes is described in equation (2.6). In addition to

pressure drop for laminar flow there will also be a head loss (pressure

drop) caused by the airflow going into the pipes. The coefficient of

discharge C_d is defined as the ratio of actual flow volume and the

theoretical flow volume. In this case C_d is consider to be 1 as the flow

paths are close together. The head loss can be calculated using equation

(2.7). And the total pressure drop would be the summation of laminar

pressure drop plus head loss described as equation (2.8) [5].

Laminar Pressure Drop $$\Delta P_L = \frac{32\mu\, L\, \dot{V}}{A\, D_h{}^2}$$ (2.6)

Head loss $$\Delta P_O = \frac{\rho\, \dot{V}^2}{2(C_d\, A)^2}$$ (2.7)

Total Pressure Drop $\Delta P_T = \Delta P_L + \Delta P_O$ (2.8)

In addition to numerical results a wind tunnel test was taken for one

battery pack. Figure 2-5 illustrates a flow experiment being taken. Figure

2-6 shows the combined results of numerical and experimental data. The

blue curve representing numerical data is accurate compare to the results

of flow test. Using the same numerical method the total pressure drop of

three battery packs can be determined shown in Figure 2-7.
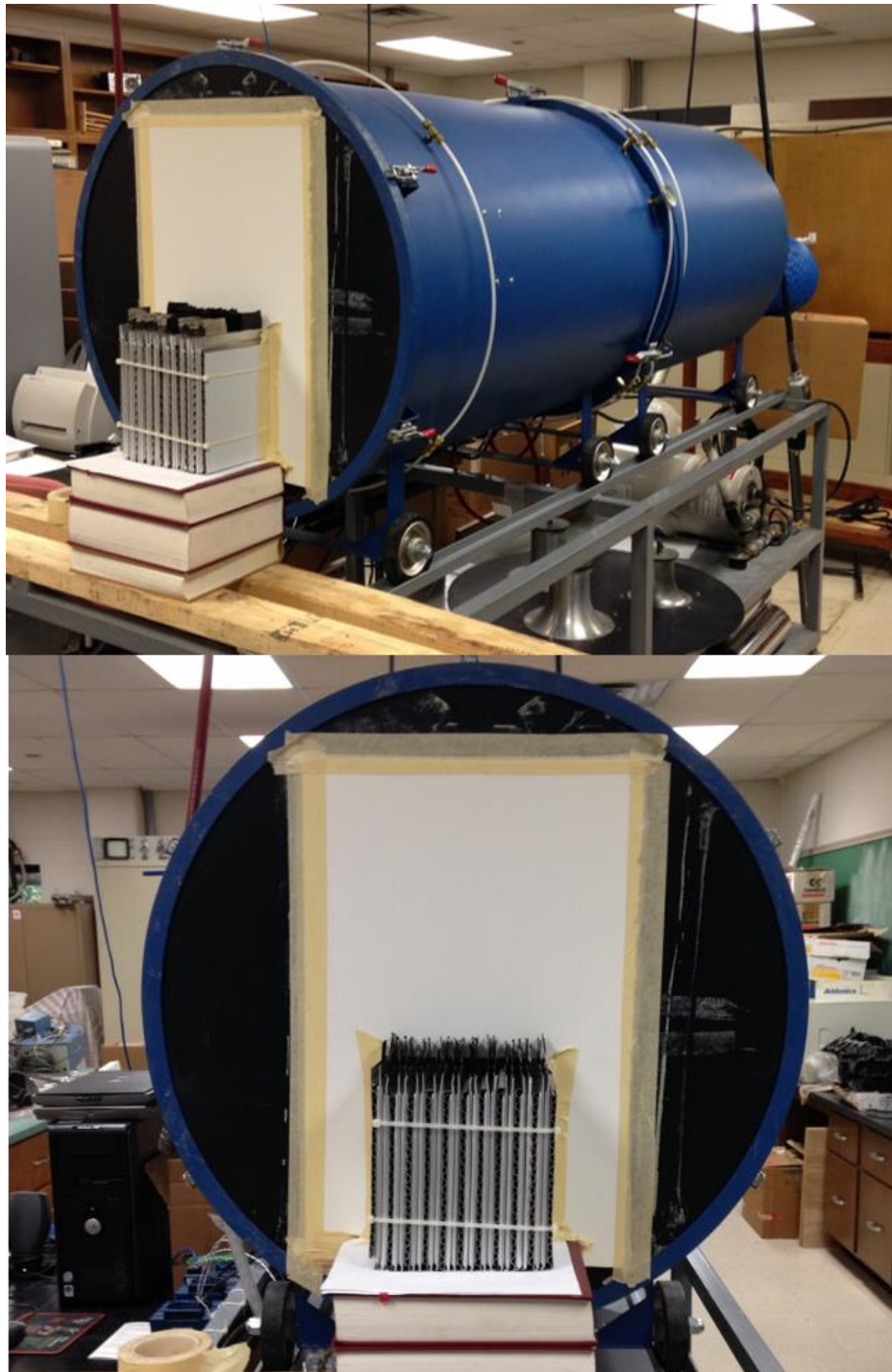
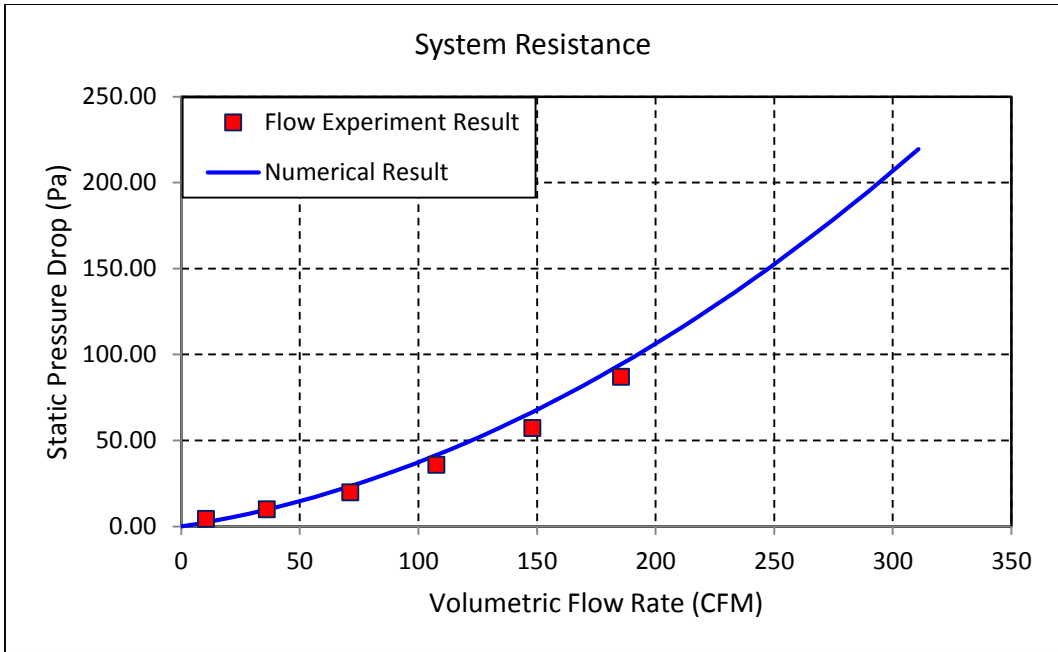Figure 2-5 Flow Experiment on Battery Pack

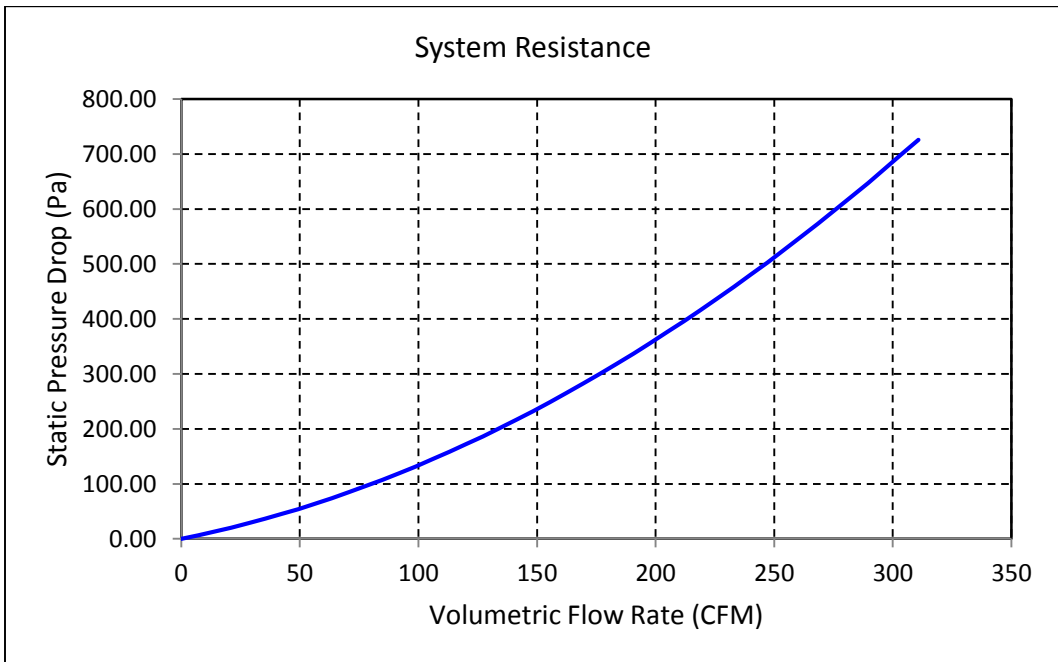Figure 2-6 System Resistance Curve of One Battery Pack

Figure 2-7 System Resistance Curve of Three Battery Packs

Chapter 3

Cooling Fans

3.1 Fan Performance curve

It is a crucial task to choose the most efficient cooling fan for the

system. Based on the demand of team electrical engineers, only 12V DC

fans can be used for the system. All of the 12V DC fans on the market

were researched for this design in order to choose the best. And fan

performance curve, shown in Figure 3-1, provided by the manufactures is

the most important guidance for choosing a cooling fan.
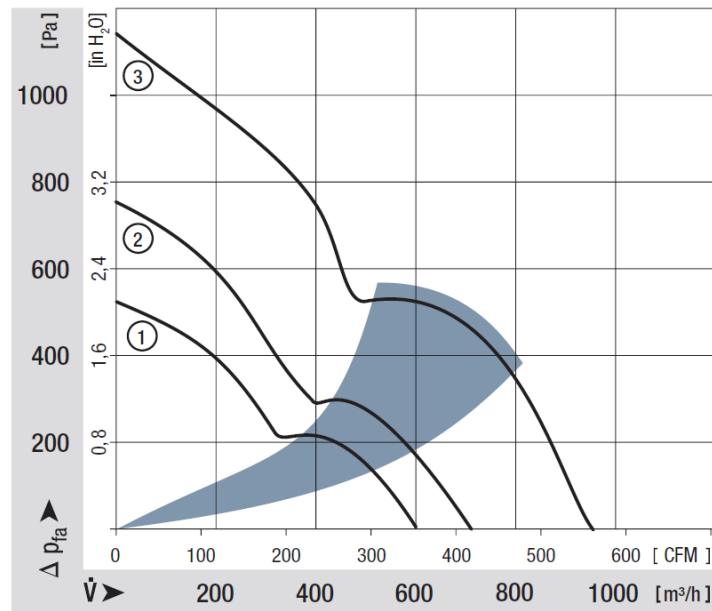
Figure 3-1 Example of Performance Curve of Three Different Fans

The fan performance curve is essentially a static pressure curve

constructed by plotting multiple static pressure points versus specific

volumetric flow rates at a given test speed, providing basis for flow and

pressure calculation [2]. The static pressure curve depicting the

performance of the fan at a given speed can also be used to determine

the pressure capability.
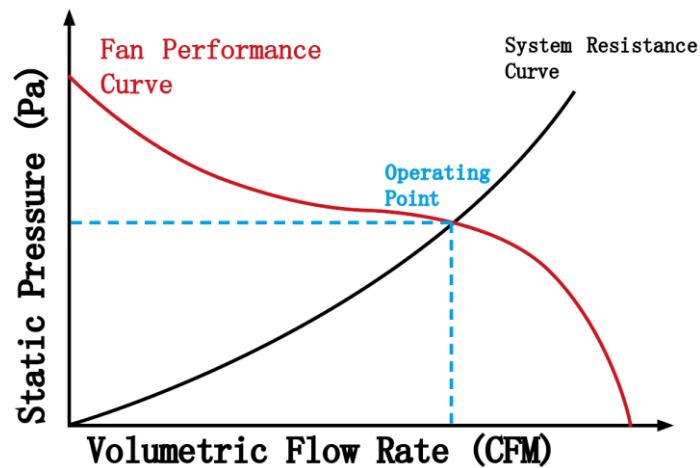
Figure 3-2 Fan Performance Curve with System Resistance Curve

Figure 3-2 illustrates, to locate the point of operation for a certain

fan and a given system the fan performance curve and the system

resistance curve have to be overlapped together. And the intersection

point would be the operating point which will determine how fast the air

flow is moving and how much pressure the air flow has to overcome.

To understand fan performance curve one can always consider a

torque versus revolution curve for an electric motor as shown in Figure 3-

3.

For an electric motor the highest revolution and peak torque can never occur at the same time. The higher the revolution goes the lower the torque becomes. In a similar way, the performance data provided by the fan manufactures always include the highest volumetric flow rate the fan can provided and the highest pressure the fan can overcome but they never occur at the same time. As the flow rate increase the pressure will decrease.
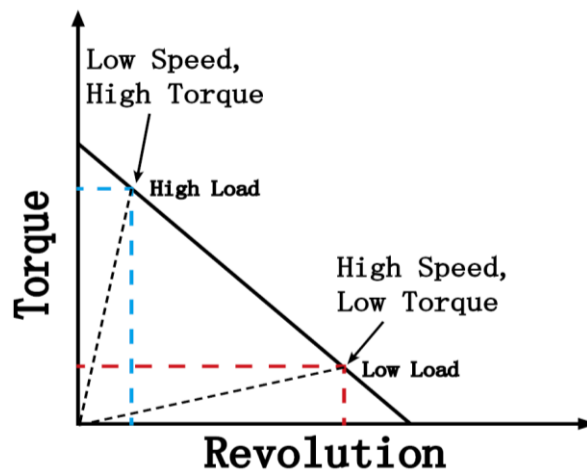

Figure 3-3 Torque VS Revolution

How to choose a fan for a given system is highly dependent on the load or to be more specific the system resistance curve. Fans are often divided into two categories high pressure fans and high speed fans for different load scenario as shown in Figure 3-4 and Figure 3-5.

For a high system resistance, a high pressure fan can actually provide more airflow than a high speed fan despite the name high speed.

And for a low system resistance a high speed fan can really provide more
airflow.
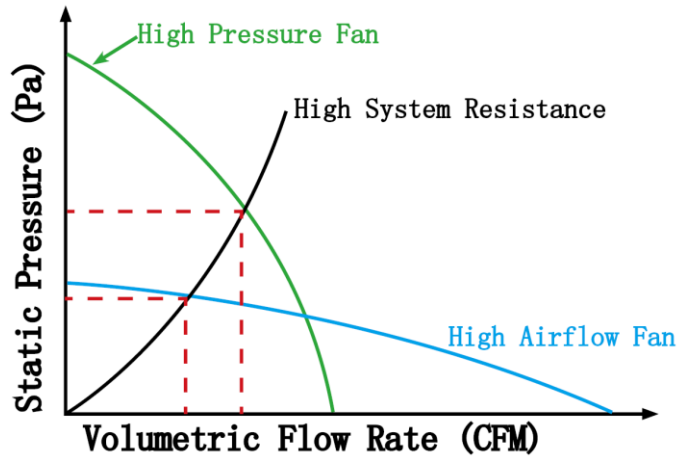
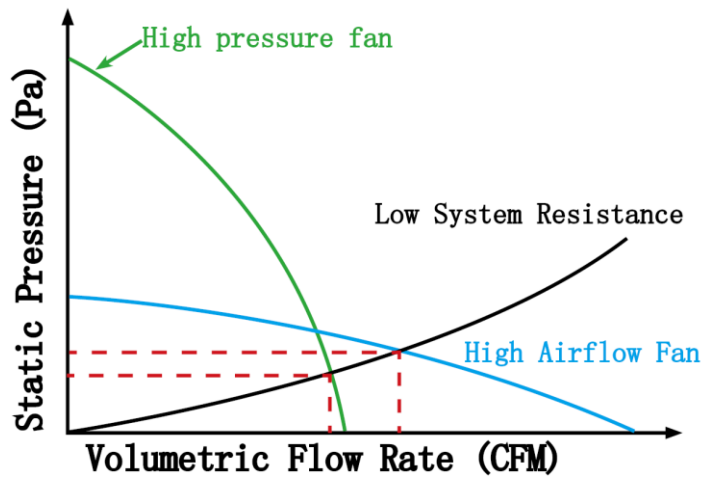Figure 3-4 High System Resistance Curve

Figure 3-5 Low System Resistance Curve

3.2 Comparison on Fans

There are two types of fans on the current market, axial fans and
centrifugal fans. Both of them have distinctive features and function

differently. Therefore each of them is suited for different applications and working environments [5]. Figure 3-6 shows comparison of fan performance curves between a centrifugal fan and an axial fan.
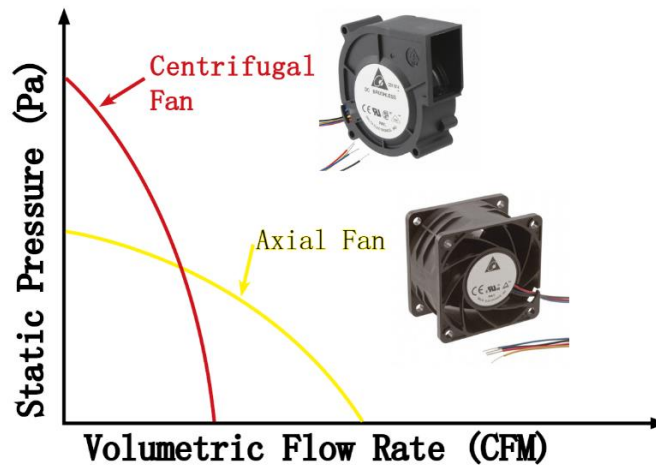
Figure 3-6 Blower Compare to Axial Fan

Centrifugal fans are often called blowers and they function differently from axial fans. The pressure of an airflow is increased by a fan wheel, a circular hub with multiple blades. Centrifugal fans move air radially which means the direction of the airflow is changed, usually by ninety degrees with respect to the direction of the incoming flow. The flow inside of a centrifugal fan is directed through a series of ducts or tubes, which will help create a higher pressure than axial fans. Centrifugal fans can provide a more steady flow but also require higher power input.

Axial fans are named for the direction of the flow. Fan blades rotates around an axis to draw air in parallel to the axis and to force air out

in the same direction. Axial fans can create higher flow rate compare to centrifugal fans meaning moving larger volume of airflow.

A similar comparison among axial fans is that an axial fan with a larger diameter can generate higher flow and small axial fan can generate higher pressure much like a blower as shown in Figure 3-7.
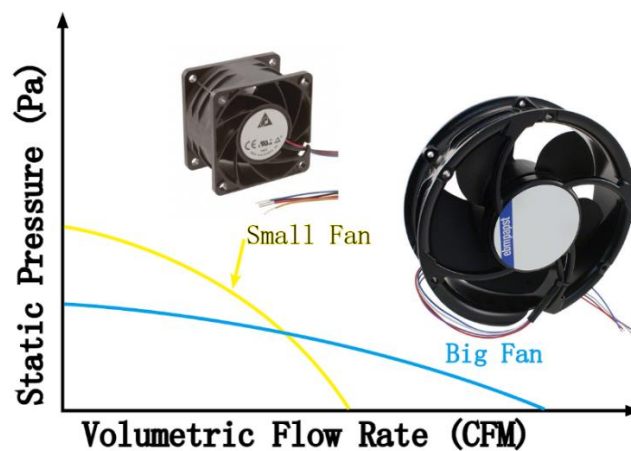

Figure 3-7 Small Axial Fan Compare to Big Axial Fan

3.3 Multiple Fan System

Fans can be combined in series or in parallel to improve the performance [6]. Two smaller fans are often less expensive than one large fan. Fans putting in series tend to be suitable for systems with long ducts and high static pressure drop across the components. Fans used in an induced configuration can minimize the amount of pressurization in a duct of an enclosure. Fans in series has advantages including lower duct

pressure, lower noise generation and less structural and electrical support requirements.

On the other hand, parallel fan configuration can be feasible for systems that has large changes in air moving directions. Wide variations in system demand prevent a single fan from consistently operating close to highest efficiency. Multiple fans in parallel enable units to be energized incrementally to meet the demands for a given system.

In simple words, putting two identical fans in series can generate twice as much static pressure as a single fan while maintaining the same air flow rate. And putting two identical fans in parallel will generate twice as much airflow and maintaining the same static pressure as shown in Figure 3-8 and Figure 3-9.
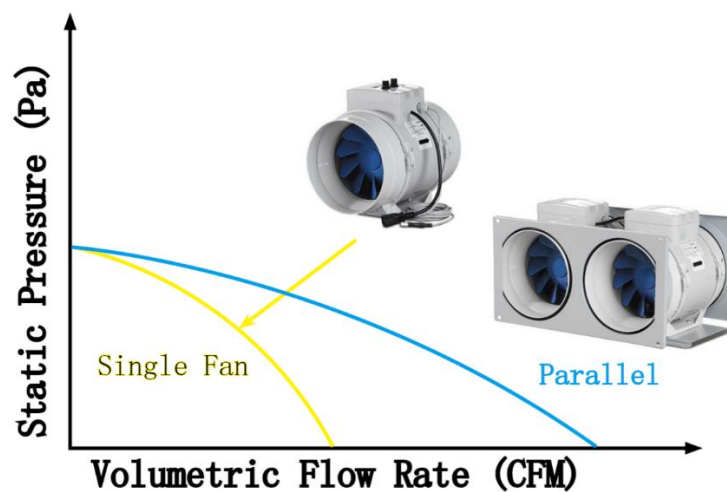
Figure 3-8 Parallel Configuration
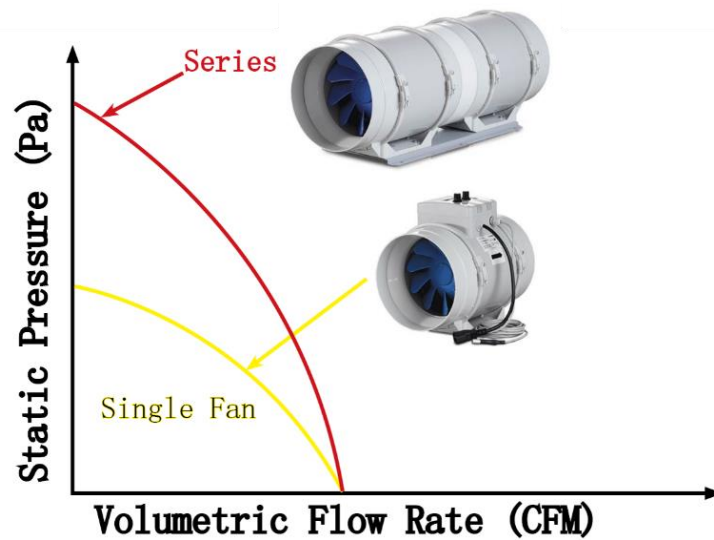
Figure 3-9 Series Configuration

3.4 Fan Choice

Although using multiple fans has advantages in cooling performance, the complexity for wire packaging will inevitably be increased shown in Figure 3-10. And also more components can potentially cause more problems in the race.
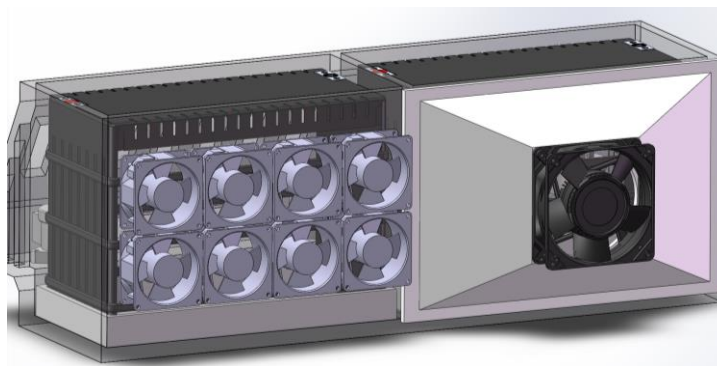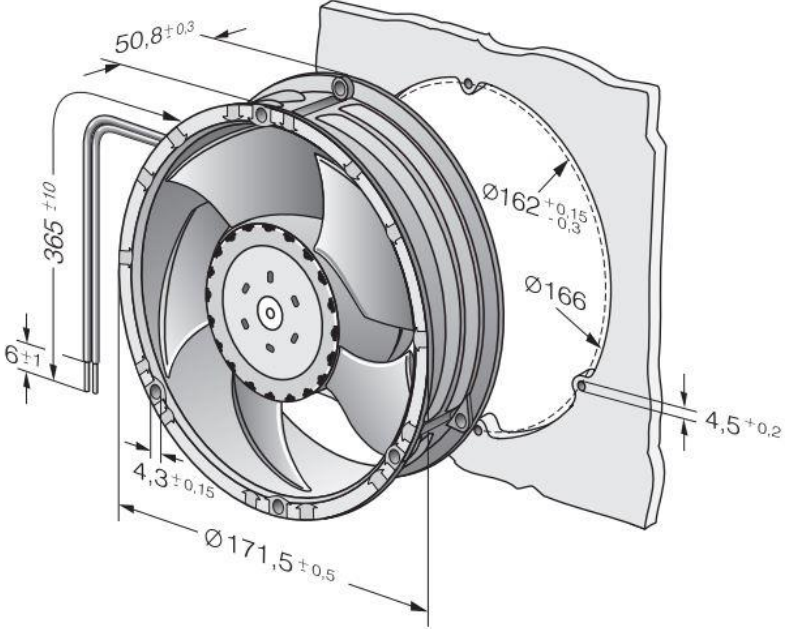

Figure 3-10 Multiple Fans Compare to Single Fan

In order to keep the system simple and reliable, a single fan system was chosen which is manufactured by a prestigious German manufacture ebm-papst with performance data and dimensions shown in Table 3.1.

Table 3.1

Manufacture	ebm-papst
Part Number	6312 /2 TDHP
Mass	0.91kg
Nominal Voltage	12V DC
Power Input	40W
Performance Data	350CFM, 520Pa
Dimensions	172 Ø x 51 mm

Chapter 4 Thermal Simulation and Conclusions

In chapter two system resistance curve was calculated for one battery pack. Using the same method the system resistance curve for three packs can be calculated as well. Combining it with the fan performance curve from chapter three the operating point for the system can be determined. The operating point is where the system resistance curve and the fan performance curve intersect, shown in Figure 4-1.
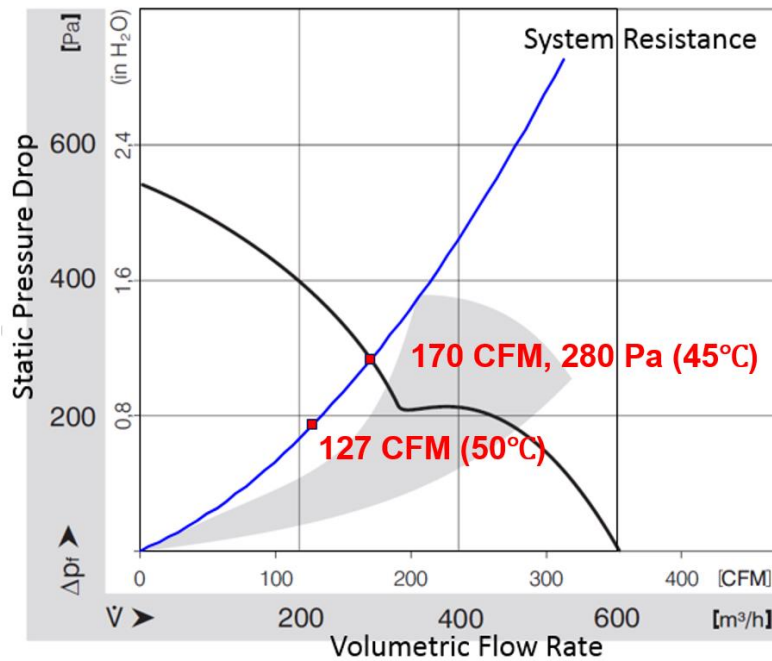
Figure 4-1 Operating Point

Figure 4-1 shows at the operating point the fan will deliver 170 CFM overcoming 280 Pa of pressure which is higher than the least required volumetric flow rate of 127.14 CFM, a desirable result.

With current data a thermal simulation can be generated using
ANSYS Icepak. First, fan curve and fan geometry was imported into the
model as shown in Figure 4-2 and Figure 4-3 [7]. The fan is placed at the
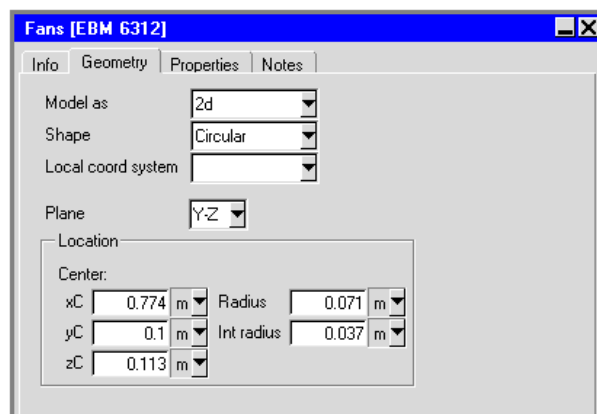exit of the flow.
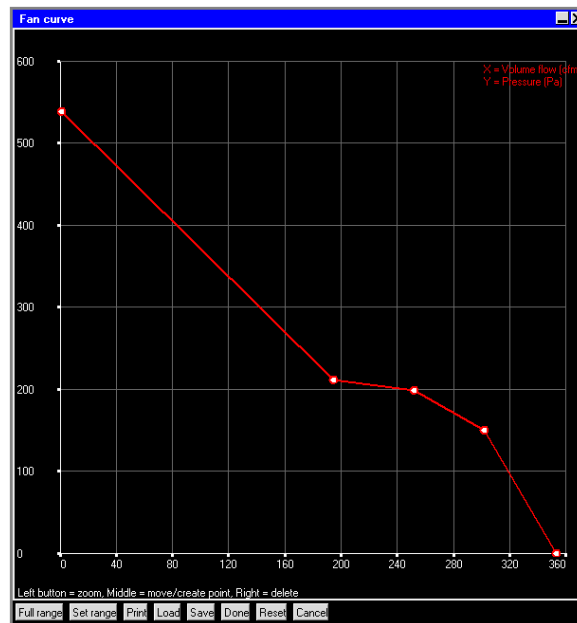
Figure 4-2 Importing Fan Curve

Figure 4-3 Fan Geometry

Second, battery packs are created using block feature. Each block represents two battery cells. Each block has 40W of heat dissipation and also the same thermal conductivity. Figure 4-4 shows battery thermal conductivity being defined. Noting that battery conductivity is different for each direction.
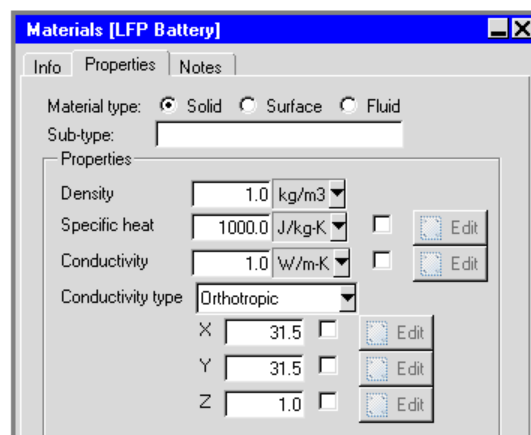
Figure 4-4 Battery Thermal Conductivity

Since generating trapzoidal tube is difficult square tubes are used to simulate the corrugation shown in Figure 4-5.
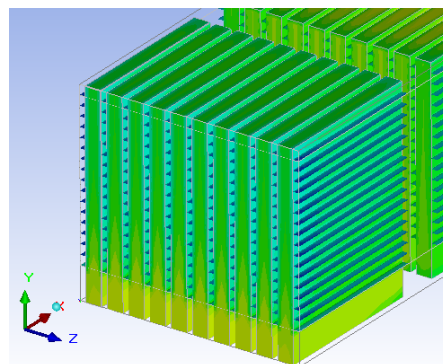
Figure 4-5 Battery Pack Model

In order to achieve a comprehensive results, the simulation was run under both laminar and turbulent flows and compared to draw the conclusions.
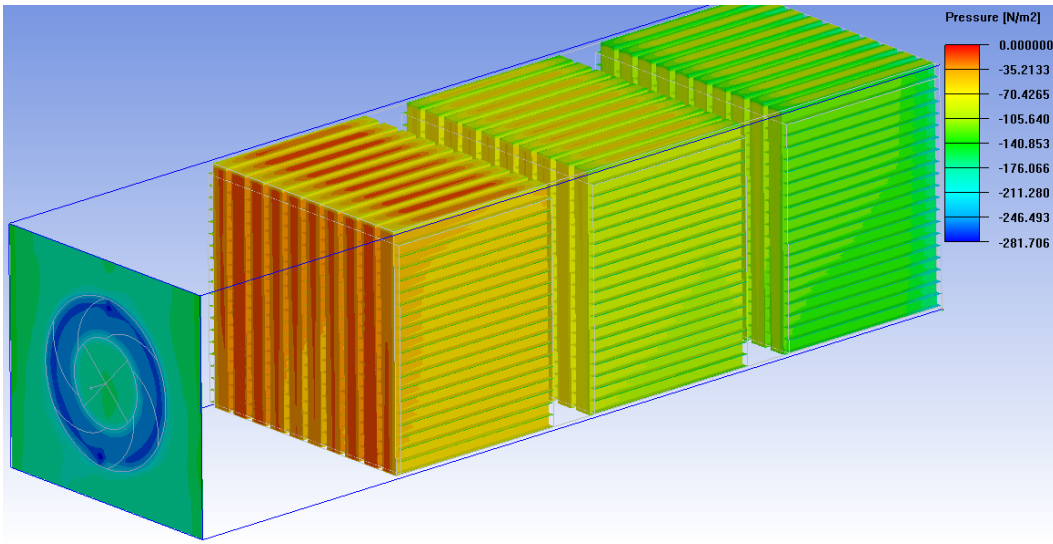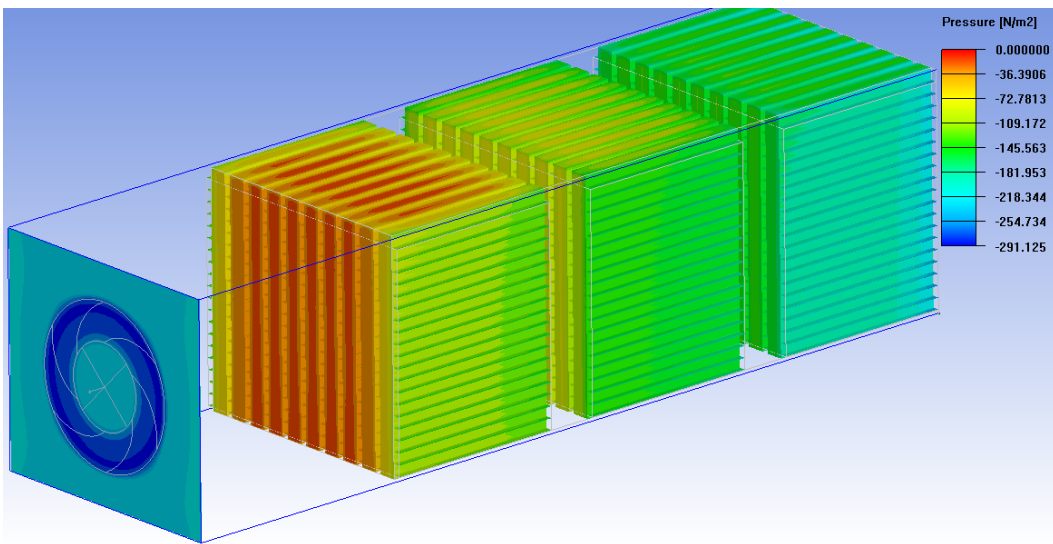

Figure 4-6 Pressure Drop (Laminar)

Figure 4-7 Pressure Drop (Turbulent)

Figure 4-6 shows the result of the pressure profile. The highest negative pressure occors at the fan which is 276. According to Figure 4-1 the pressure drop based on the operating point should be 280 Pa. The results are close. Figure 4-7 illustrates the pressure drop under turbulent flow which is 288 Pa. The turbulent flow creats more resistance therefore higher pressure drop.
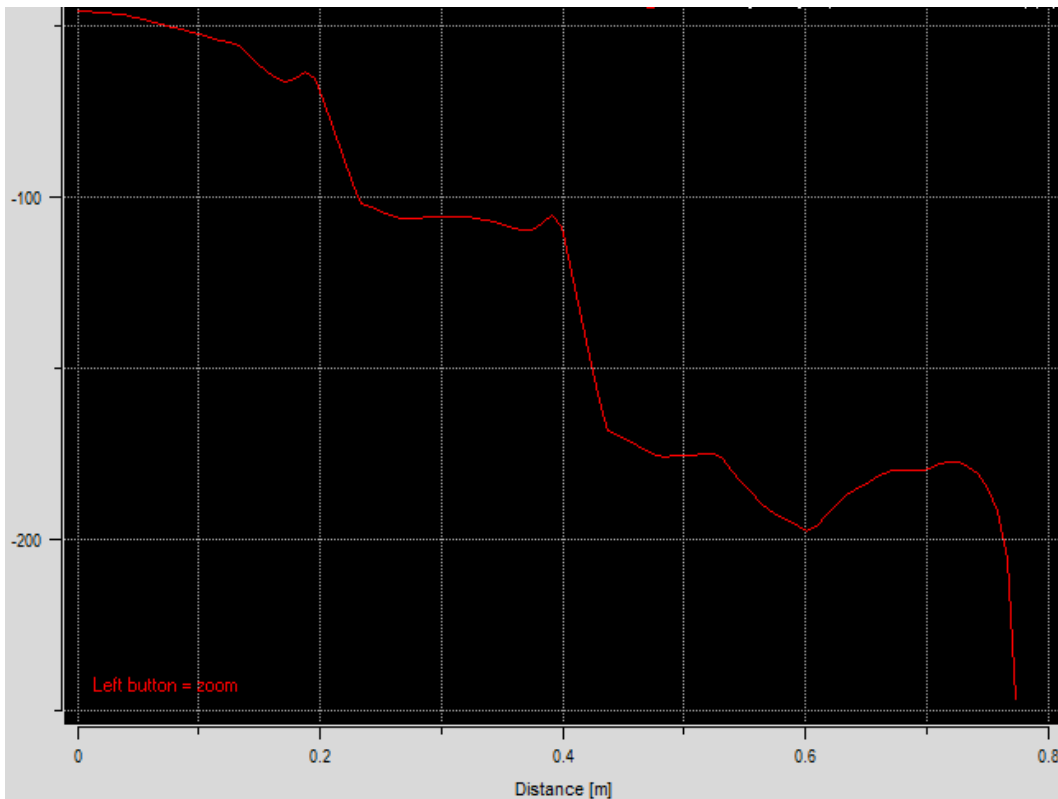

Figure 4-8 Pressure Drop across One Channel (Laminar)

Figure 4-8 and Figure 4-9 show pressure drop across one channel under laminar and turbulent flow. The pressure decrease gradualy from the entrance to the exit and the negative pressure reach its peak at the

exit. In both laminar and turbulent condition the flow experience

disturbances when the flow is leaving one battery pack and entering

another one. In general the two curves are similar despite that turbulent

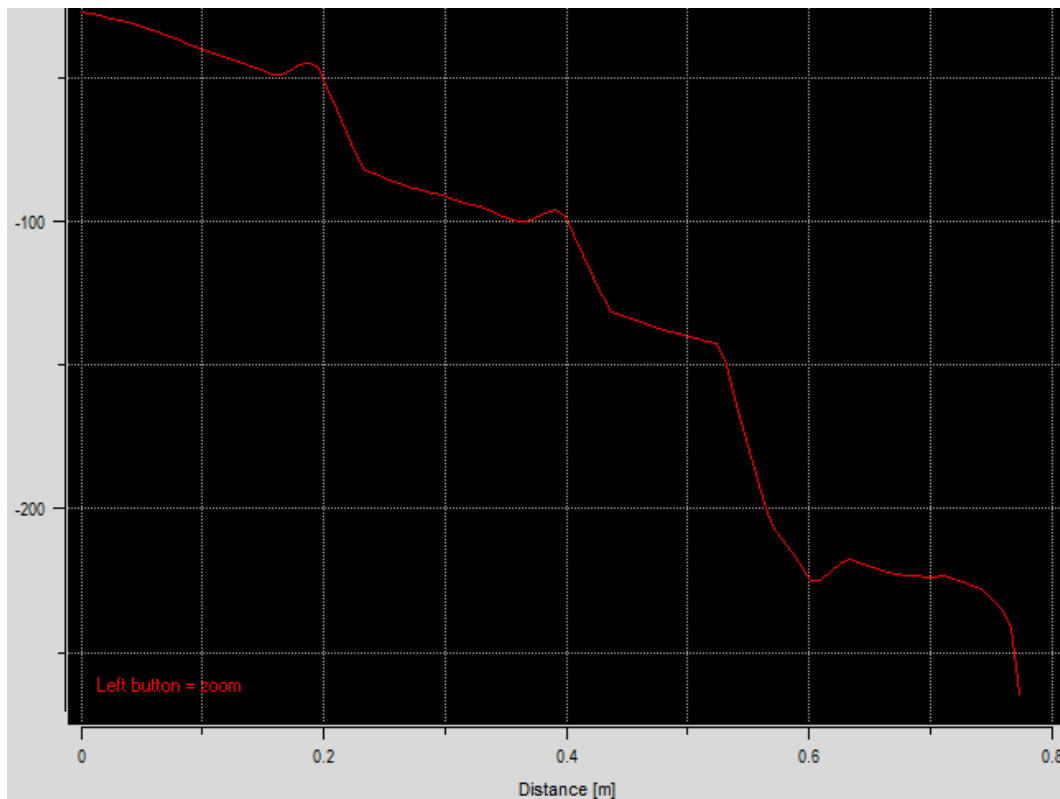flow creates more pressure drop.

Figure 4-9 Pressure Drop across One Channel (Turbulent)

Using the flow rate from the operating point the flow velocity can be

calculated which is 8 m/s at the exit of the flow region. For laminar flow the

flow velocity is 13.2 m/s according to simulation, shown in Figure 4-10

vertical cross section area. And for turbulent flow the flow velocity is 8.25

m/s, shown in Figure 4-11. Interestingly the simulation result under

turbulent flow is closer to the calculation result despite the fact that laminar

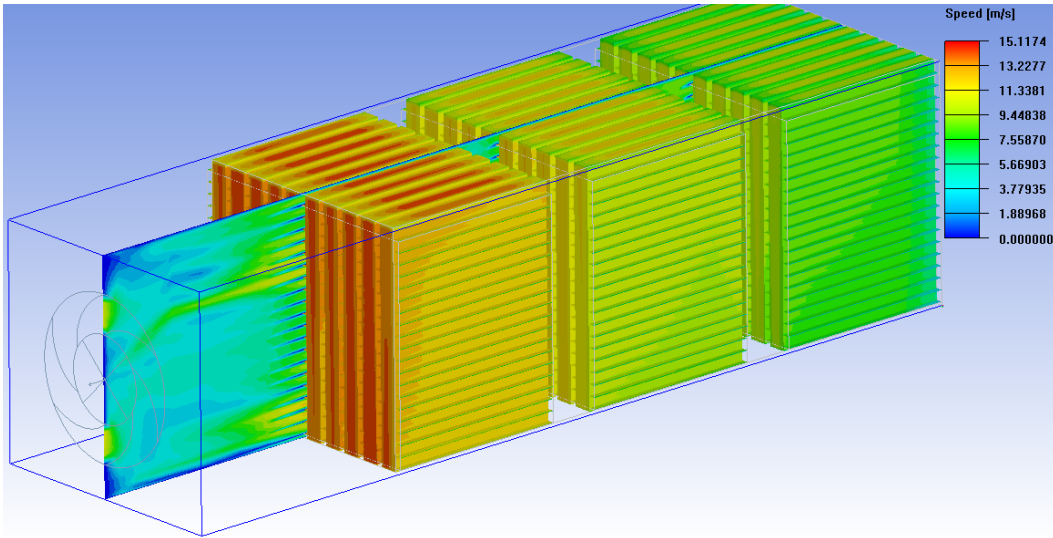equation was used in the calculation.

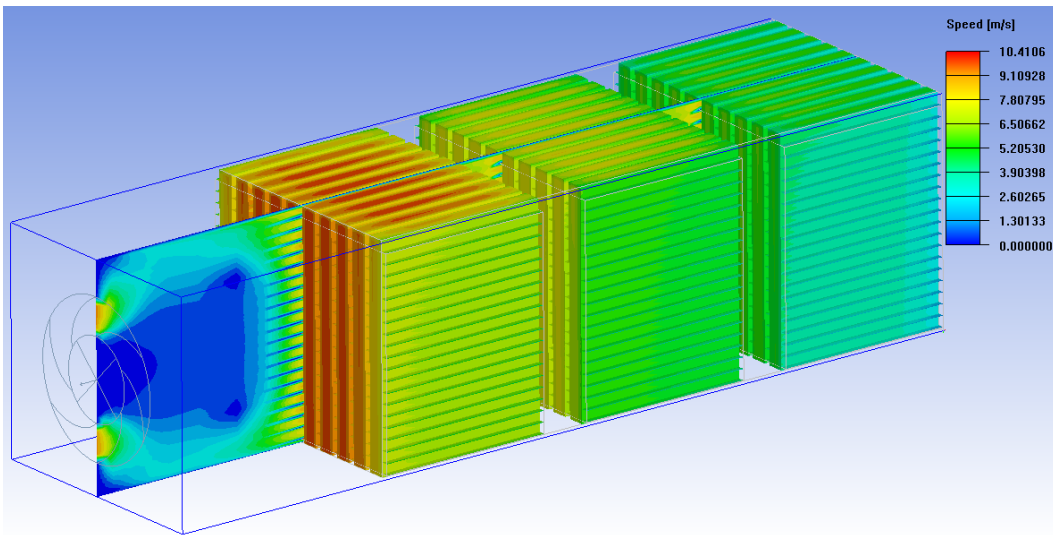Figure 4-10 Flow Velocity (Laminar)
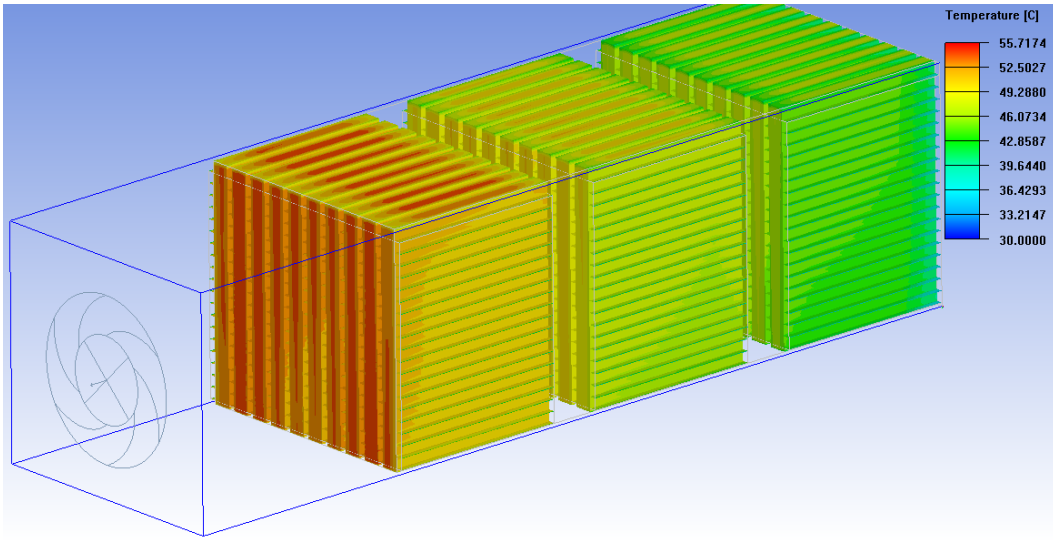

Figure 4-11 Flow Velocity (Turbulent)

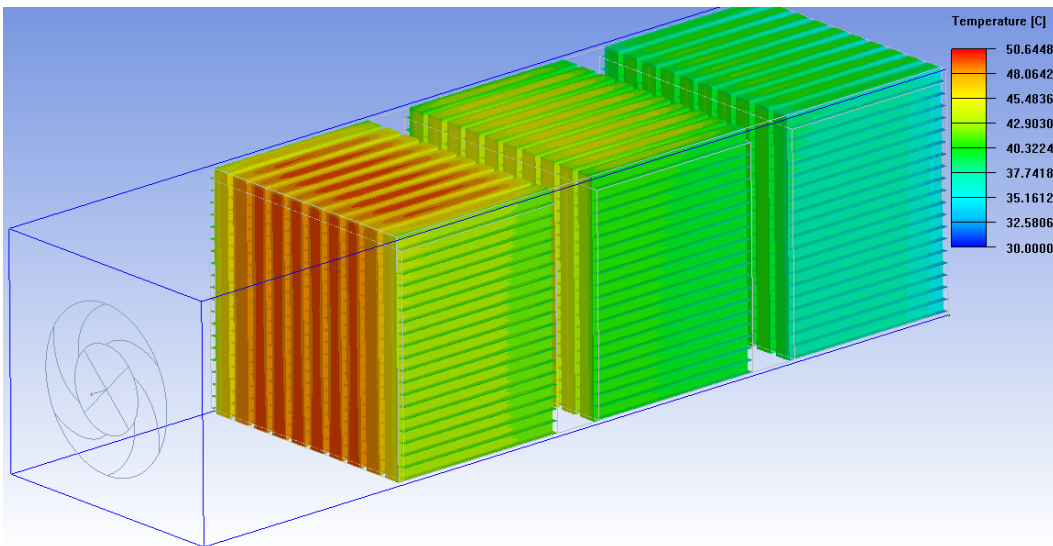Figure 4-12 Cell Temperature (Laminar)

Figure 4-13 Cell temperature (Turbulent)

The cell temperature is eventually the most important result since the whole purpose was to keep the batteries from overheating. By intuition one can speculate that the three battery pack will not be at the same

temperature the one at the entrance should be the coolest and the one near the exit should be the hottest. But in the calculation the progression was not taken into account therefore the temperature calculated was actually the average temperature among the three pack. And what really matters is not the average but the peak temperature of all three packs. Figure 4-12 and Figure 4-13 show that under laminar flow the cell temperature averaging at 49℃ and 43.2℃ respectively. Regarding peak temperature, under laminar flow the highest cell temperature is 55.7℃ and under turbulent flow the highest cell temperature is 50.6℃.
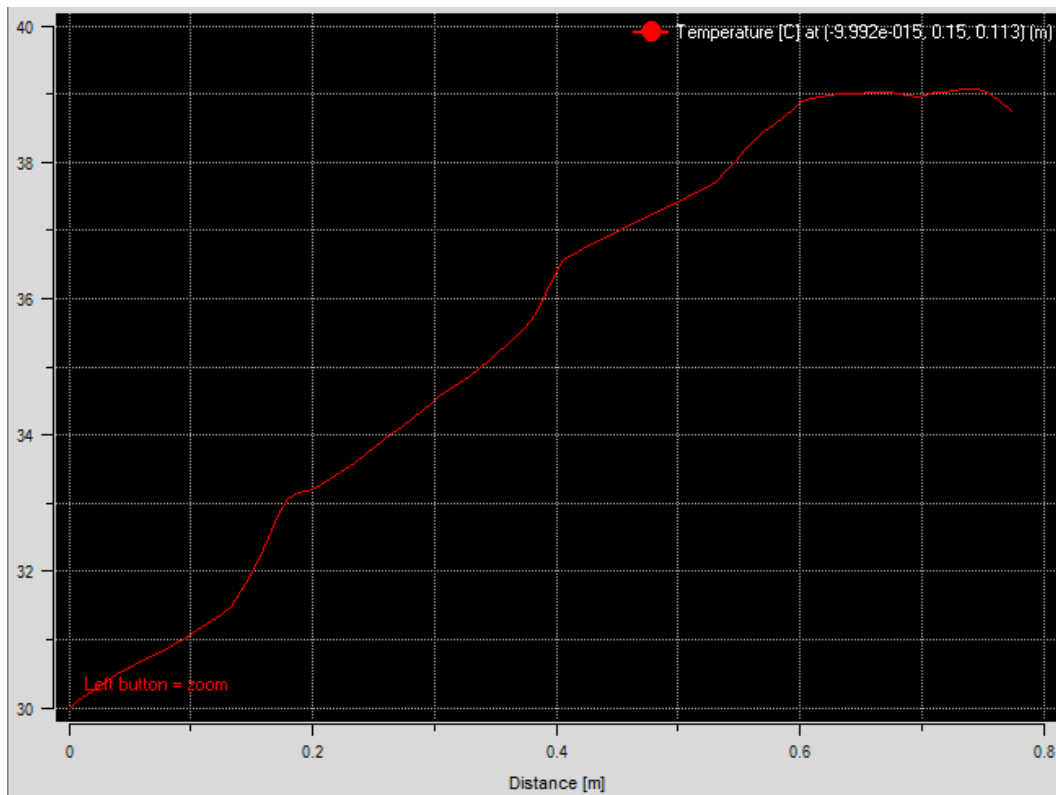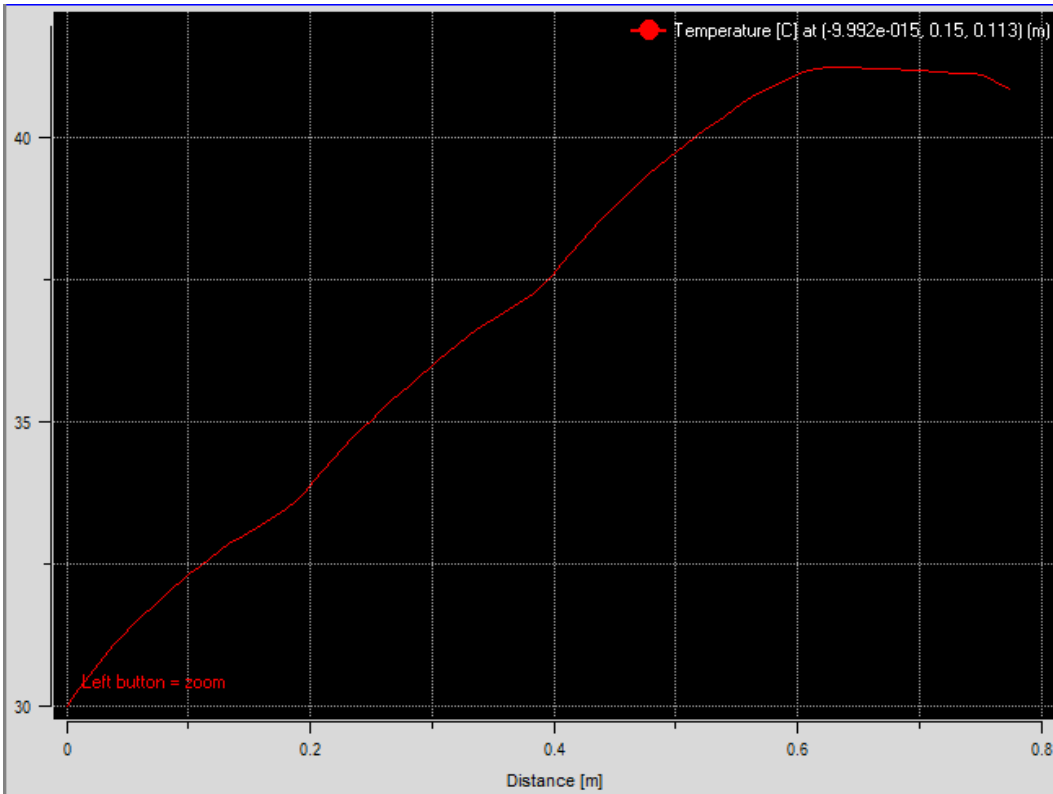

Figure 4-14 Air Temperature (Laminar)

Figure 4-15 Air Temperature (Turbulent)

In conclusion, compare to laminar flow turbulent flow generates more resistance and higher pressure drop therefore has less flow rate. However, turbulent flow does create more convection which can be seen from the fact that the air temperature is higher under turbulent flow, which can be seen from Figure 4-14 and Figure 4-15 measured with respect to distance. The way to improve the cooling performance of the system would be creating more turbulence in the system which can be achieved by increasing the surface roughness and increasing the hydraulic diameter of the tunnels.

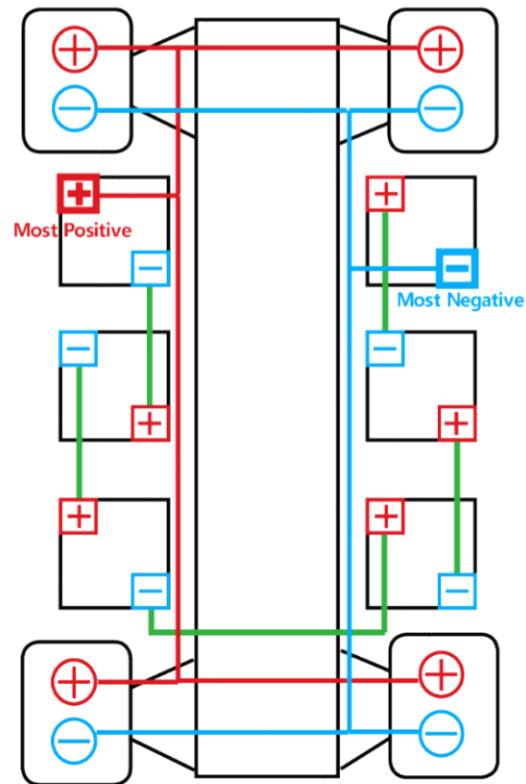Appendix A

Illustration of Accumulators
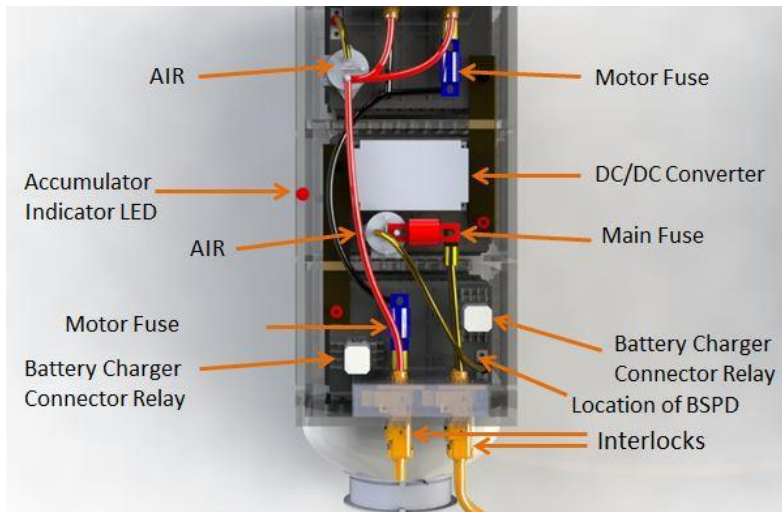
Figure A-1 Battery Layout

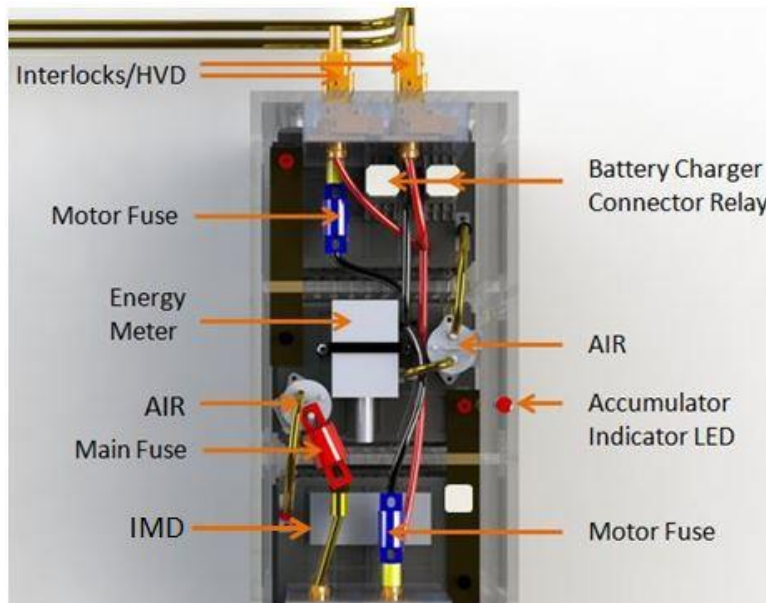Figure A-2 Left Accumulator Components
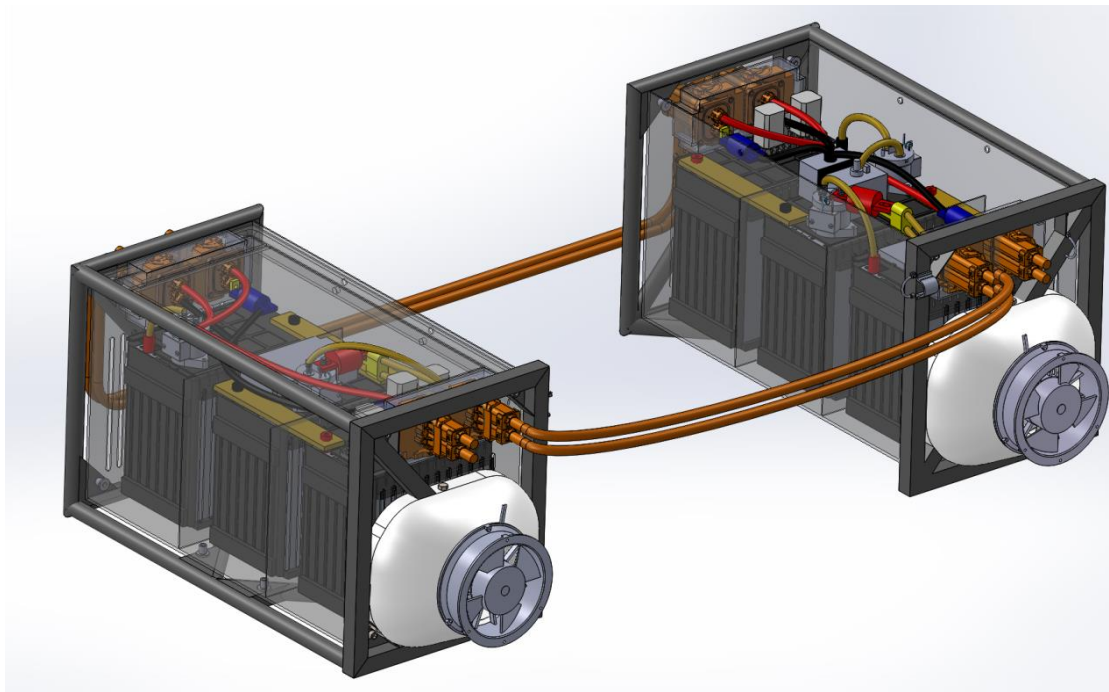
Figure A-3 Right Accumulator Components

Figure A-4 SolidWorks Models of Accumulators

References

[1] S. Reineman, "Design and Analysis of a Battery for a Formula Electric Car," Massachusetts Institute of Technology, 2013.

[2] S. Mathewson, "Experimental Measurements of LiFePO4 Battery Thermal Characteristics," University of Waterloo, Waterloo, Ontario, Canada, 2014.

[3] Y. A. Cengel, Heat Transfer: A Practical Approach, Mcgraw-Hill, 2002.

[4] Y. A. Cengel, Introduction to Thermodynamics and Heat Transfer, McGraw-Hill, 2007.

[5] "Formula SAE Rules," Society of Automotive Engineering, 2016.

[6] R. L. W. a. K. L. Lawrence, Modeling and Simulation of Dynamic Systems, Prentice Hall, 1997.

[7] U. D. o. Energy, "Improving Fan System Performance," 2003.

[8] ebmpapst, "Using Fans in Series and Parallel: Performance Guidelines," ebmpapst, 2016.

[9] I. ANSYS, "ANSYS Icepak Tutorials," 2013. [Online]. Available: http://148.204.81.206/Ansys/150/ANSYS%20Icepak%20Tutorials.pdf.

[10] M. Hibbard, "UTA Racing Electrical Safety Form," 2015.

Biographical Information

Yin earned his Bachelor of Engineering in Vehicle Engineering from Beijing Information Science & Technology University, Beijing, China. He participated in the Formula SAE competition in China as the chief engineering in his undergraduate program.

He joined UTA Racing in 2014. As a design lead he worked on cooling and packaging of accumulators for E-16 Electric car. He earned his Master of Science in Mechanical Engineering from University of Texas at Arlington in 2016.